

Intrusion Detection in Wireless Sensor Networks for Destructive Intruders

Qixiang Yu, Zhenxing Luo, and Paul Min
 Department of Electrical and Systems Engineering
 Washington University in St. Louis St. Louis, MO, 63130
 Email: (yuqixiang, mariolzx, psm)@wustl.edu

Abstract—Intrusion detection in a wireless sensor network (WSN) has drawn intensive attentions recently due to its wide applications. Many issues in intrusion detection, such as sensor deployment, mobility of sensors and data fusion have been investigated extensively. However, the behavior of the intruder has rarely been investigated. In this paper, we introduce a novel situation where the intruder can destroy encountered sensors. This situation is analyzed theoretically and experimentally under our system model. The key point is to discuss the intrusion detection problem differently according to the speed of the intruder. We derive the detection probability, which can be applied to any sensor deployment utilizing the disc model. The detection model we used includes a single-sensing detection model and a multiple-sensing detection model. Some interesting factors in intrusion detection, such as transmission period, sampling period, and the random entrance time of the intruder are also considered. Finally, our Monte-Carlo simulation results validated our analytical results.

Keywords—wireless sensor network, intrusion detection, disc model, destructive intruder

I. INTRODUCTION

Nowadays, it is economically feasible to manufacture a large quantity of small and low-cost sensors. Since these sensors are highly flexible, survivable, stable, and effective, WSNs are suitable for many applications, such as battlefield surveillance, traffic monitoring, and fire detection [1]. This paper investigates the application of WSNs in intruder detection.

In the intruder detection problem, based on the information from sensors, the WSN tries to determine the presence of an intruder in a region of interest (ROI). Intruder detection has been studied intensively [2]-[6]. Many factors can influence the detection performance, such as sensor distribution, sensor type, sensor positions, detection model and intrusion strategy. In [2], authors studied the effect of different sensor distributions on the detection performance. Particularly, the authors in [2] used a single-sensing detection model and a multiple-sensing detection model. In [3], the authors investigated the effect of sensor types on intruder detection. Moreover, sensors can move as in [5] to provide better field coverage and the presented detection algorithm does not depend on a particular sensor field shape. In this paper, however, we only study fixed sensors because our sensors are low-cost and not able to move. Furthermore, only homogeneous sensors are used in this paper to simplify our analysis. Particularly, we investigate the new situation where the intruder can destroy sensors it encounters based on the setup in [2][3]. To the best of our knowledge, no one has studied this situation before. We will also consider

some uninvestigated factors, such as random intruder entrance time, random sensor destruction and transmission period.

Our main contributions are listed below. First, we considered a new intrusion detection problem in which the intruder could destroy all sensors in its surrounding region for the single-sensing detection model and the multiple-sensing detection model. Second, we investigated the effect of the transmission period on detection performance. Third, the effects of the random intruder entrance time and the random destruction strategy were also discussed. Finally, simulations were carried out to validate our analytical results.

The rest of this article is organized as follows. In Section II, the system model we used is presented, followed by the intrusion detection method in Section III. The effect of the transmission period and the sampling period is discussed in Section IV where we evaluate the problem using the single-sensing detection model. In section V, the multiple-sensing detection model is considered and some new conditions are presented in Section VI. Simulation results are presented and discussed in Section VII. Finally, concluding remarks are given in Section VIII.

II. SYSTEM MODEL

Similar to the models in [2][3], our system model consists of a sensing and detection model, a network deployment model, an intrusion strategy model, and evaluation metrics. The sensing and detection model specifies the way the system detects the intruder. In this paper, we use the single-sensing detection model and the multiple-sensing detection model. The network model defines the sensor field layout and sensor configurations. The intrusion strategy model defines the movement of the intruder. The evaluation metrics describe the metrics used to assess the intrusion detection performance. We use the disc model in [4] in our analysis since it is practical and appropriate for our configurations.

A. Sensing and Detection Model

In this paper, we analyze the intrusion detection problem using the single-sensing detection model and the multiple-sensing detection model. The intruder is detected when it is identified by a single sensor in the single-sensing model or when it is identified by m sensors in the multiple-sensing detection model where m depends on the particular application. Please note that these m sensors need not to sense the intruder at the same time under the multiple-sensing detection model.

Obviously, the detection probability obtained by using the

multiple-sensing detection model is less than that obtained by using the single-sensing detection model in the same WSN. However, the multiple-sensing detection model may be useful in some applications. For example, the collected data from one sensor may be insufficient if we want to estimate the intruder position. Information from at least three sensors is needed for position estimation if sensors are not able to measure the direction of incoming signals [7][8]. In this particular instance, the intruder can be successfully detected and located only by using multiple-sensing detection models. In this paper, we use both detection models.

B. Network Deployment Model

The WSN used in this paper consists of N sensors deployed in a two-dimensional coordinate system. Before the intruder appears, these sensors are deployed in a square area $A = L \times L$, where L is the side length. All sensors are stationary after deployment. A sensor can only detect the intruder within its sensing coverage area, which is a disk of radius r_s . Moreover, all sensors have the same sensing range. Besides the sensing range, the probability to identify an intruder, called identification probability, is also important. The identification probability can be described as a function g , which can be a boolean function or a probability function whose argument can be the distance between the sensor and the intruder. If a boolean function is used, we assume that the intruder will be immediately identified after entering the sensing area of a sensor. In other cases, whether the intruder will be identified is determined by the identification function, which will be explained later.

In this paper, we discuss a WSN with N sensors randomly deployed around a target point (i.e., the center of the ROI) following a particular distribution. This distribution can be a two-dimensional uniform distribution or a two-dimensional Gaussian distribution [3]

$$f(x, y, \sigma) = \frac{1}{2\pi\sigma^2} e^{-\frac{x^2+y^2}{2\sigma^2}} \quad (1)$$

where the parameter σ is the standard deviation. There are other deployment strategies with mixing normal distributions, i.e., hybrid gaussian-ring deployment [9] and k-gaussian deployment [10]. In the following analyses, we use the distribution function $f_{xy}(\sigma)$ to represent a general function for the sensor deployment in a Cartesian coordinate system. Therefore, our derivation is valid for all sensor deployments.

Moreover, we assume that sensors can transmit signals to the fusion center with period T and there is no emergency transmission or asynchronous transmission (Fig. 1). Delay is also an essential factor in the intrusion detection. It can be caused by the acoustic signal propagation delay or by the sensor sampling interval. We do not take the sampling interval into consideration since it is insignificant compared to the transmission period. Furthermore, acoustic signal propagation delay is omitted since it does not affect our derivation.

C. Intrusion Strategy Model

Similar to the setup in [2], we assume that the intruder has the knowledge of the target location. Since we do not take landform into consideration, invading in a straight-line path is regarded as the most efficient intrusion strategy. Under our hypothesis, the intruder can enter the ROI from an arbitrary

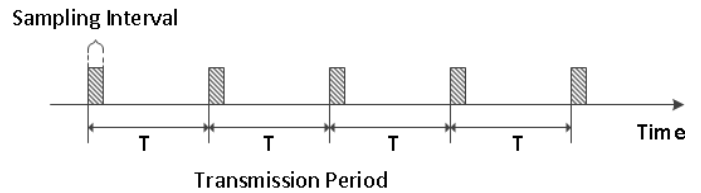


Fig. 1. Sampling Interval

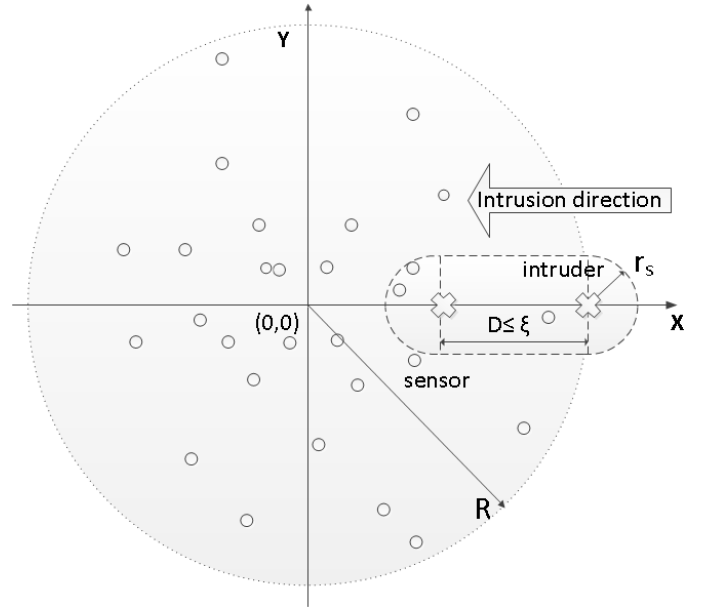


Fig. 2. Intrusion detection area in a WSN with intrusion distance $D = \xi$

point with distance R to the target. Then, it goes directly to the target in a straight line with velocity V . We can build the Cartesian coordinate system based on the intrusion path (Fig. 2).

As explained in the introduction section, we also consider the situation where the intruder destroys sensors along its path. The destruction region has a certain radius. The intruder will immediately destroy all sensors in its destruction region. In other words, we assume that no time interval exists between sensor destructions and that the number of destroyable sensors is not limited. Further assumptions will be made and clarified during the derivation.

D. Evaluation Metrics

The following two metrics are useful to evaluate intrusion detection [3]. The first metric is intrusion distance D . It is the distance that the intruder advances before it is detected by the WSN. The second metric is the detection probability $P[D \leq \xi]$. It is the probability that an intruder can be detected before reaching the maximal allowable intrusion distance ξ . The detection probability is the primary metric we use to measure the detection performance in this paper.

III. INTRUSION DETECTION IN A WSN

A significant difference between our research and previous research is that in our research, the intruder can destroy all sensors in its surrounding region with radius r_d . In this paper, we assume that the sensor detection distance r_s is larger than r_d . Otherwise, the intruder will never be detected under our

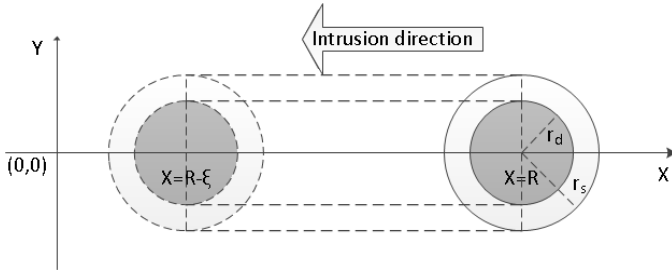


Fig. 3. Intrusion detection using the disc model

assumption.

In the given network model, there are N sensors deployed inside the ROI. Based on Theorem 1 in [2], a similar theorem using our assumptions is presented. The transmission period is not taken into consideration here. A detailed proof, which is based on the proof in [2], is also provided.

Theorem 1: Suppose the maximal allowable intrusion distance for a given WSN is ξ ($\xi \geq 0$), and the intruder starts at point $(R, 0)$ while the target stays at point $(0, 0)$. Let $P_1[D \leq \xi]$ denote the detection probability that the intruder can be detected within the maximal allowable intrusion distance under the single-sensing detection model. The detection probability is

$$\begin{aligned}
 P_1[D \leq \xi] = & 1 - \left\{ 1 - \int_{R-\xi}^R \int_{-r_s}^{r_s} f_{xy}(\sigma) dy dx \right. \\
 & - \int_{R-\xi-r_s}^{R-\xi} \int_{-\sqrt{r_s^2-(x-R+\xi)^2}}^{\sqrt{r_s^2-(x-R+\xi)^2}} f_{xy}(\sigma) dy dx \\
 & - \int_R^{R+r_s} \int_{-\sqrt{r_s^2-(x-R)^2}}^{\sqrt{r_s^2-(x-R)^2}} f_{xy}(\sigma) dy dx \\
 & + \int_{R-\xi}^R \int_{-r_d}^{r_d} f_{xy}(\sigma) dy dx \\
 & + \int_{R-\xi-r_d}^{R-\xi} \int_{-\sqrt{r_d^2-(x-R+\xi)^2}}^{\sqrt{r_d^2-(x-R+\xi)^2}} f_{xy}(\sigma) dy dx \\
 & \left. + \int_R^{R+r_d} \int_{-\sqrt{r_d^2-(x-R)^2}}^{\sqrt{r_d^2-(x-R)^2}} f_{xy}(\sigma) dy dx \right\}^N \quad (2)
 \end{aligned}$$

where $f_{xy}(\sigma)$ stands for the probability density function (PDF) of the sensor distribution.

Proof: In order to calculate the intrusion detection probability, a Cartesian coordinate system is used as illustrated in Fig. 2 and Fig. 3. Without loss of generality, point $(0, 0)$ is set as the location of the target, and point $(R, 0)$ is the starting position of the intruder. The intruder is moving toward the target in a straight line, along the x-axis. Once the entrance point is fixed, the corresponding Cartesian coordinate system can be built accordingly.

As the intruder would be detected within the distance ξ in the single-sensing detection model, there should be at least one sensor located in the corresponding detection region S_ξ . The area of S_ξ is given by $S_\xi = 2\xi r_s + \pi^2 r_s^2$ as illustrated in Fig. 3. The small circles in Fig. 3 indicate the destruction region of the intruder. Sensors within the large circles can detect the intruder.

Let p_s be the probability that a sensor is deployed in the

large rectangular region and the two half discoidal regions. Let p_d be the probability that a sensor resides in the small rectangular region and the two small half discoidal regions. We can calculate p_s and p_d by integration:

$$\begin{aligned}
 p_s = & \int_{R-\xi}^R \int_{-r_s}^{r_s} f_{xy}(\sigma) dy dx \\
 & + \int_{R-\xi-r_s}^{R-\xi} \int_{-\sqrt{r_s^2-(x-R+\xi)^2}}^{\sqrt{r_s^2-(x-R+\xi)^2}} f_{xy}(\sigma) dy dx \\
 & + \int_R^{R+r_s} \int_{-\sqrt{r_s^2-(x-R)^2}}^{\sqrt{r_s^2-(x-R)^2}} f_{xy}(\sigma) dy dx \quad (3)
 \end{aligned}$$

$$\begin{aligned}
 p_d = & \int_{R-\xi}^R \int_{-r_d}^{r_d} f_{xy}(\sigma) dy dx + \\
 & \int_{R-\xi-r_d}^{R-\xi} \int_{-\sqrt{r_d^2-(x-R+\xi)^2}}^{\sqrt{r_d^2-(x-R+\xi)^2}} f_{xy}(\sigma) dy dx + \\
 & \int_R^{R+r_d} \int_{-\sqrt{r_d^2-(x-R)^2}}^{\sqrt{r_d^2-(x-R)^2}} f_{xy}(\sigma) dy dx. \quad (4)
 \end{aligned}$$

Then, the probability p_ξ that a sensor is deployed in the region where it can detect the intruder and will not be destroyed can be expressed as $p_\xi = p_s - p_d$. The probability that there is no sensor located in the detection region is $1 - p_\xi$. Thus, the probability that there is at least one sensor located in that region can be expressed as $1 - (1 - p_\xi)^N$. It is obvious that $P_1[D \leq \xi]$ should equal to $1 - (1 - p_\xi)^N$. Hence, we have equation (2). ■

Note that ξ equals 0 means that the intruder is immediately detected when it enters the ROI. We denote $P_1[D = 0]$ as the instant detection probability [3].

IV. CASE ANALYSIS FOR THE SINGLE-SENSING DETECTION MODEL

In this section, we include the transmission period in the calculation of the detection probability. We assume that the intruder appears at time 0, which is right before the time when the sensors start sampling and transmitting data. The position of the intruder is $(R - nVT, 0)$ where n represents the number of transmission periods and n is a natural number. The problem is discussed in five different cases based on the speed of the intruder, V .

We also assume that the sampling period is the same as the transmission period. In order to ensure that the data is fresh for every transmission, the sampling period is usually equal or less than the transmission period. To simplify our analysis, we set the sampling period equal to the transmission period for the rest of the paper.

In addition, we take the identification function into consideration. This function introduces the situation where the intruder is in the detection region but it is not identified by sensors. This is related to the signal strength received by the sensors, which is a distance function. In sum, the identification function generates the probability that a sensor identifies the intruder within its sensing range based on the distance between them. The identification function at time nT is denoted by $g_{xy}(nT)$. Therefore, we use $f_{xy}(\sigma)g_{xy}(nT)$ to represent the

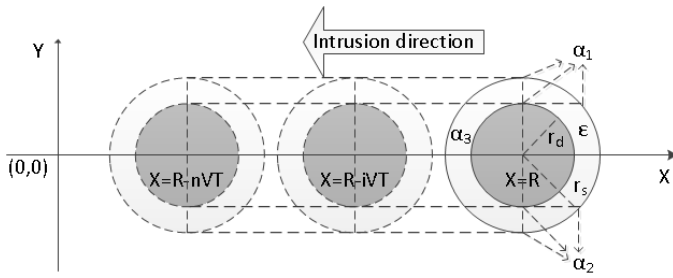


Fig. 4. Intrusion detection using the disc model: case one

probability that the sensor at the point (x, y) detects the intruder at time nT .

In following cases, the detection probability is calculated using the disc model. In other words, the calculation is based on the disc size rather than the entire area that the intruder travels through. Thus, the integration over the rectangle in Eqn. (2) will be replaced with the sum of integrals over parts of the discs.

A. Case One

In this case, we assume that $V \geq \frac{2r_s}{T}$ so that the detection discs do not overlap each other. Hence, the detection probability $P_2[D \leq nVT]$ is

$$P_2[D \leq nVT] = 1 - \left\{1 - \sum_{i=0}^n p_\alpha(i) - p_\epsilon\right\}^N \quad (5)$$

where

$$p_\alpha(i) = \int_{R-iVT}^{R-iVT+} \int_{\sqrt{r_s^2-r_d^2}}^{\sqrt{r_s^2-(x-R+iVT)^2}} f_{xy}(\sigma) g_{xy}(iT) dy dx + \int_{R-iVT}^{R-iVT+} \int_{-r_d}^{-\sqrt{r_s^2-(x-R+iVT)^2}} f_{xy}(\sigma) g_{xy}(iT) dy dx + \int_{R-iVT-r_s}^{R-iVT} \int_{-\sqrt{r_s^2-(x-R+iVT)^2}}^{\sqrt{r_s^2-(x-R+iVT)^2}} f_{xy}(\sigma) g_{xy}(iT) dy dx - \int_{R-iVT-r_d}^{R-iVT} \int_{-\sqrt{r_d^2-(x-R+iVT)^2}}^{\sqrt{r_d^2-(x-R+iVT)^2}} f_{xy}(\sigma) g_{xy}(iT) dy dx, \quad (6)$$

$$p_\epsilon = \int_{-r_d}^{r_d} \int_{R+\sqrt{r_d^2-y^2}}^{R+\sqrt{r_s^2-y^2}} f_{xy}(\sigma) g_{xy}(iT) dx dy. \quad (7)$$

In equation (6), the first term stands for the probability that a sensor, which detects the intruder, exists in every intercepted top-right area of the detection discs, i.e., area α_1 (Fig. 4). Similarly, the second term stands for the probability that a sensor exists in every intercepted bottom-right area of the detection discs, i.e., area α_2 . The third term represents the probability that a sensor exists in every left semicircle of the detection discs. The last term represents the probability that a sensor exists in every left semicircle of the destruction disc. By subtracting the last term from the third term, we will get the probability of the left parts of rings, i.e., area α_3 . Although some parts of the half rings are inside the small rectangle formed by destruction regions, the sensor stays undamaged at

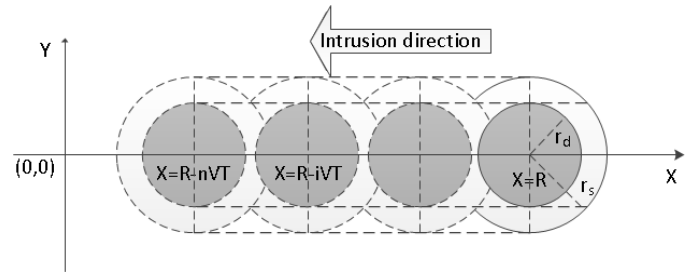


Fig. 5. Intrusion detection using the disc model: case two

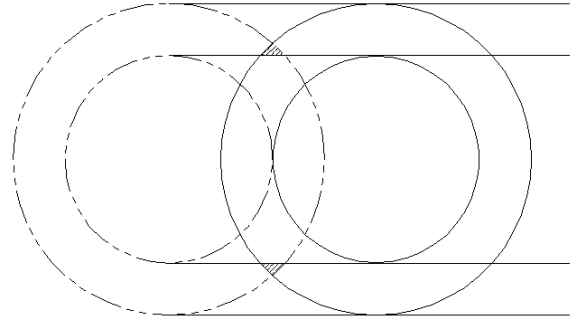


Fig. 6. Intrusion detection using the disc model: case three

the time of sampling. Therefore, we still calculate the detection probability using the whole left parts of the rings.

Eqn. (7) indicates the probability that a sensor exists in the area ϵ , which is the area of the rightmost ring between $[-r_d, r_d]$ on the y-axis. We do not consider the corresponding areas of other discs since the sensors in those areas would have been destroyed by the intruder before the sampling time. Thus, the sum of equation (6) and equation (7) is the probability that one sensor identifies the intruder. Therefore, we can get Eqn. (5) based on the proof of Theorem 1.

B. Case Two

In case two, we assume that $\frac{2\sqrt{r_s^2-r_d^2}}{T} < V < \frac{2r_s}{T}$. In this case, the top areas of the detection disc (the part of the rings that does not stay in the smaller rectangular region) do not lay over their previous detection areas (Fig. 5). Eqn. (5) still works here since there is no overlap between the actual detection areas. We choose the boundaries based on our calculation category. It does not matter whether $\frac{2r_d}{T}$, whose geometrical meaning is the destruction discs tangent to the next destruction discs, belongs to this case.

C. Case Three

In this case, we have $\frac{\sqrt{r_s^2-r_d^2}}{T} < V < \frac{2\sqrt{r_s^2-r_d^2}}{T}$, which means that there are overlaps of the actual detection areas in our previous calculation (Fig. 6). Thus, the detection probability can be calculated as

$$P_2[D \leq nVT] = 1 - \left\{1 - \sum_{i=0}^n p_\alpha(i) + \sum_{i=1}^n p_\beta(i) - p_\epsilon\right\}^N \quad (8)$$

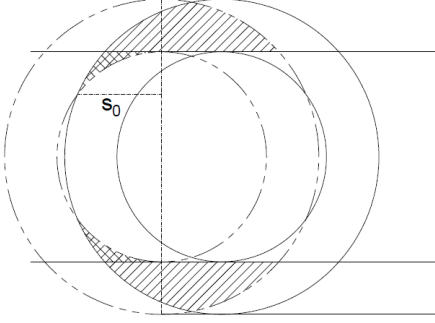


Fig. 7. Intrusion detection using the disc model: case four

where $p_\beta(i)$ equals

$$\begin{aligned}
 & \int_{R-(i-\frac{1}{2})VT}^{R-iVT} \int_{r_d}^{\sqrt{r_s^2-(x-R+iVT)^2}} f_{xy}(\sigma)g_{xy}(iT)dydx + \\
 & \int_{R-(i-\frac{1}{2})VT}^{R-iVT} \int_{-\sqrt{r_s^2-(x-R+iVT)^2}}^{-r_d} f_{xy}(\sigma)g_{xy}(iT)dydx + \\
 & \int_{R-(i-1)VT}^{R-(i-\frac{1}{2})VT} \int_{r_d}^{d_\beta} f_{xy}(\sigma)g_{xy}(iT)dydx + \\
 & \int_{R-(i-1)VT}^{R-(i-\frac{1}{2})VT} \int_{-d_\beta}^{-r_d} f_{xy}(\sigma)g_{xy}(iT)dydx \quad (9)
 \end{aligned}$$

where d_β is $\sqrt{r_s^2 - (x - R + (i - 1)VT)^2}$. In Eqn. (9), the integral limit $R - (i - \frac{1}{2})VT$ is the abscissa of the intersection of two detection circles. It is obvious that $p_\beta(i)$ equals the detection probability that a sensor exists in the hatched areas that are the overlaps on the top/bottom of detection discs. We subtract it since it is counted twice in Eqn. (5) in this case.

D. Case Four

We assume $\frac{r_s - r_d}{T} \leq V \leq \frac{\sqrt{r_s^2 - r_d^2}}{T}$ in this case. This interval means that the intersection of the destruction disc and the previous detection disc is on the left side of the detection disc (Fig. 7). The detection probability becomes

$$\begin{aligned}
 P_2[D \leq nVT] = \\
 1 - \left\{ 1 - \sum_{i=0}^n p_\alpha(i) + \sum_{i=1}^n (p_\beta(i) + p_\gamma(i)) - p_\epsilon \right\}^N \quad (10)
 \end{aligned}$$

where $p_\gamma(i)$ equals

$$\begin{aligned}
 & \int_{R-(i-1)VT}^{R-iVT} \int_{d_\gamma}^{r_d} f_{xy}(\sigma)g_{xy}(iT)dydx + \\
 & \int_{R-(i-1)VT}^{R-iVT} \int_{-r_d}^{-d_\gamma} f_{xy}(\sigma)g_{xy}(iT)dydx + \\
 & \int_{R-iVT-s_0}^{R-(i-1)VT} \int_{d_\gamma}^{d_\beta} f_{xy}(\sigma)g_{xy}(iT)dydx + \\
 & \int_{R-iVT-s_0}^{R-(i-1)VT} \int_{-d_\beta}^{-d_\gamma} f_{xy}(\sigma)g_{xy}(iT)dydx \quad (11)
 \end{aligned}$$

where $s_0 = \frac{r_s^2 - r_d^2 - V^2 T^2}{2VT}$ and $d_\gamma = \sqrt{r_d^2 - (x - R + iVT)^2}$.

The horizontal distance between the leftmost point of the cross-pattern area and the center of the leftmost circle is denoted by s_0 . It is computed based on $r_d^2 - s_0^2 = r_s^2 - (VT + s_0)^2$. In Eqn. (10), the probability $p_\gamma(i)$ equals the detection probability that a sensor exists in the cross hatched areas inside the interval $[-r_d, r_d]$. We subtract $p_\gamma(i)$ because it is counted twice.

E. Case Five

When $V < \frac{r_s - r_d}{T}$, the intruder moves so slow that it can not promptly reach the boundary of the detection disc of the last transmission time. Sensors in front of the intruder may not be destroyed within one transmission period. Thus, it is possible that the intruder may be detected by the same sensor more than one time. We do not consider this situation since it seems to be impractical for an intruder.

V. MULTIPLE-SENSING DETECTION MODEL

In this section, we discuss the intrusion detection problem using the multiple-sensing detection model. We assume that the number of sensors needed to detect the intruder is m . Similar to Theorem 2 in [2], the detection probability in the case $V \geq \frac{2r_s}{T}$ is

$$P_m = 1 - \sum_{i=0}^{m-1} \binom{N}{i} (1-p)^{(N-i)} p^i \quad (12)$$

where

$$p = \sum_{i=0}^n p_\alpha(i) - p_\epsilon. \quad (13)$$

Eqn (13) represents the probability that the intruder is within the sensing area of a sensor. Hence,

$$\sum_{i=0}^{m-1} \binom{N}{i} (1-p)^{(N-i)} p^i \quad (14)$$

represents the probability that there are no more than $m-1$ sensors, which can detect the intruder. The proof of this equation is similar to the proof of theorem 2 in [3]. When $\frac{\sqrt{d_t^2 - d_k^2}}{T} < V < \frac{2\sqrt{d_t^2 - d_k^2}}{T}$ or $\frac{d_t - d_k}{T} \leq V \leq \frac{\sqrt{d_t^2 - d_k^2}}{T}$, the detection probability is of the same form as Eqn. (12) where p equals $\sum_{i=0}^n p_\alpha(i) + \sum_{i=1}^n p_\beta(i) - p_\epsilon$ or $\sum_{i=0}^n p_\alpha(i) + \sum_{i=1}^n (p_\beta(i) + p_\gamma(i)) - p_\epsilon$.

VI. CONDITION MODIFICATION

In this section, we explore two condition modifications based on our previous analysis. One is that the intruder does not enter the WSN at time 0. The other is that the intruder does not always destroy sensors.

A. Random Entrance Time

If the intruder arrives randomly during $(0, T]$, the intruder can not be immediately detected when it enters the ROI. This is because the intruder avoids the first sampling interval. Thus, the detection probability corresponding to the same intrusion distance will decrease. Instead of the detection probability corresponding to the instant detection, the detection probability corresponding to the minimal intrusion distance is used. It has the same form as $P_2[D \leq \xi]$ where ξ is replaced with the minimal intrusion distance if the single-sensing detection model is used. If the intruder arrives at t_0 , the minimal intrusion distance can be denoted by $d = V(T - t_0)$ and the intruder's position becomes $(R - (nT - t_0)V, 0)$ instead of $(R - nVT, 0)$ in Eqn. (3) - (11).

B. Random Destruction

Random destruction means that the intruder will randomly destroy sensors it encounters. This indicates that some sensors in the destruction region of the intruder may still survive. To illustrate this situation, we assume that the intruder destroys sensors right before every sampling time, and the destruction period is the same as the transmission period. Furthermore, we assume that sensors are definitely destroyed when they leave the destruction region. In other words, there is no sensor existing in the destruction region along the intruder's path except the current destruction disc. These assumptions guarantee that we only need to apply the random destruction to the sensors inside the detection discs. This part is discussed using the single-sensing detection model.

We only discuss the random destruction under the constraint $r_d < \sqrt{r_s^2 - r_d^2}$. Assuming that the destroying probability is p_d , we have:

a) If $\frac{2r_d}{T} < V < \frac{2\sqrt{r_s^2 - r_d^2}}{T}$, the destruction regions are not overlapped and the detection probability is

$$P_2[D \leq nVT] = 1 - \left\{ 1 - \sum_{i=0}^n (p_\alpha(i) + (1 - p_d)p_\delta(i)) + \sum_{i=1}^n p_\beta(i) - p_\epsilon \right\}^N \quad (15)$$

where $p_\delta(i)$ equals

$$\int_{R-iVT-r_d}^{R-iVT+r_d} \int_{-d_\gamma}^{d_\gamma} f_{xy}(\sigma) g_{xy}(iT) dy dx. \quad (16)$$

b) If $V < \frac{2r_d}{T}$, the destruction discs partially overlap each other. Because of the overlap, the sensors may detect the intruder more than one time. The result will be complicated if destructions in the overlapping area are not independent.

To simplify the derivation, we assume that the destructions are carried out independently. Thus, we utilize $(1 - p_d)^2$ to indicate the probability that a sensor still survives after two rounds of destruction. Therefore, the probability that a sensor survives the first round of destruction but not the second round of destruction can be expressed as $(1 - p_d)p_d$.

We use s_1 to represent the distance from the intersection points of two destruction discs to the Y-axis. Because $r_d^2 - s_1^2 = (\frac{VT}{2})^2$, we can get

$$s_1 = \sqrt{r_d^2 - \left(\frac{VT}{2}\right)^2}. \quad (17)$$

Then, we can just add the term

$$\int_{-s_1}^{s_1} \int_{R-(i-1)VT-\sqrt{r_d^2-y^2}}^{R-iVT+\sqrt{r_d^2-y^2}} f_{xy}(\sigma) g_{xy}(iT) (1 - p_d) p_d dx dy \quad (18)$$

to the second summation in Eqn. (10).

VII. RESULTS AND DISCUSSION

To validate our analytical results, we calculated the theoretical results corresponding to the single-sensing detection model as well as to the multiple-sensing detection model. Then, we compared our theoretical results with the Monte-Carlo simulation results. The Monte-Carlo simulation results were generated by averaging 10^4 simulation results. By averaging a large number of simulation results, we believe our Monte-Carlo simulation results will closely match the real experiment results.

The ROI was a square with side length $a = b = 100m$. The transmission period T was $1s$. The target was located at the center of the ROI. The intruder entered the ROI at time 0 from an arbitrary point with distance $R = 30m$ to the target. The maximum intrusion distance was set to $\xi = 0m$ for simulations of instant detection and to $20m$ for others. The destruction radius r_d was set to $1m$. In the simulations in Section VIII(A)&(B), the detection radius and the identification function were set as $r_s = 2m$ and $g_{xy}(iT) = 1$ respectively. Their values for the rest simulations are presented in Section VIII(C). After building the coordinate system, we assume that the intruder appeared at point $(R, 0)$. Then, the probability that the intruder would be detected was computed.

To calculate the analytical results, sensors were deployed according to the two-dimensional uniform distribution or the two-dimensional Gaussian distribution. The PDF of the uniform distribution was $f(x, y) = 1/ab$ where $x, y \in [-50, 50]$. The PDF of the Gaussian distribution was Eqn. (1) with $\sigma = 25$. In the Monte-Carlo simulation, sensors were deployed according to the same distributions as to those in the theoretical results.

In figures of this section, solid lines represents the analytical results and dash-dot lines represents the Monte-Carlo simulation results. The meanings of the curves are determined by the line shapes. For example, solid lines with diamonds in figures stand for the analytical results of the case one simulation when the single-sensing detection model was used and the distribution of sensors followed the gaussian distribution. Full legends can be found under Fig. 8, 12 and 13.

A. Simulation for Case One, Three and Four

In simulations corresponding to case one, we set the intruder speed to $V = 5 \text{ m/s} > \frac{2r_s}{T}$. For case three, we set the speed to $V = 2.5 \text{ m/s}$, which was in the range $[\frac{\sqrt{r_s^2 - r_d^2}}{T}, \frac{2\sqrt{r_s^2 - r_d^2}}{T}]$. For case four, we set the speed to $V = 1.5 \text{ m/s}$, which satisfied the restriction $\frac{r_s - r_d}{T} \leq V \leq \frac{\sqrt{r_s^2 - r_d^2}}{T}$. For the simulations using the multiple-sensing detection model, we set $m = 3$, which means that the intruder is identified if it is detected by three sensors.

In Fig. 8-11, all dashed lines match the corresponding solid lines, which means the Monte-Carlo simulation results validate the analytical results under the single-sensing detection model and the multiple-sensing detection model. This indicates that the equations of the detection probability we derived are

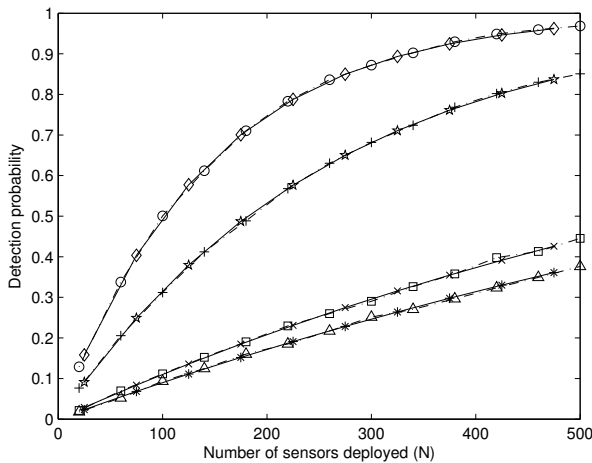


Fig. 8. Detection probability corresponding to the single-sensing detection model when $V = 5 \text{ m/s}$. Solid line+diamond: analytical $\xi = 20m$ & gaussian, solid line+pentagram: analytical $\xi = 20m$ & uniform, solid line+x-mark: analytical $\xi = 0m$ & gaussian, solid line+star: analytical $\xi = 0m$ & uniform; dashed line+circle: Monte-Carlo $\xi = 20m$ & gaussian, dashed line+plus: Monte-Carlo $\xi = 20m$ & uniform, dashed line+square: Monte-Carlo $\xi = 0m$ & gaussian, dashed line+triangle (up): Monte-Carlo $\xi = 0m$ & uniform. (The legends in Fig. 9-12 are the same as these here.)

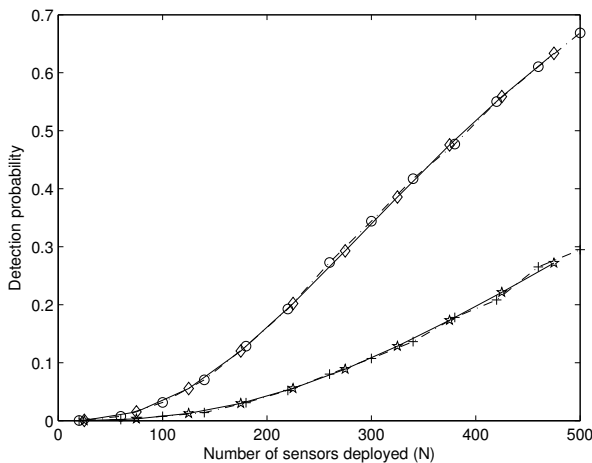


Fig. 9. Detection probability corresponding to the multiple-sensing detection model when $V = 5 \text{ m/s}$.

correct. We can also see that decreasing the speed of the intruder could increase the detection probability when the intruder travels the same distance. This is because information from more sampling periods can be used.

By comparing these results, we found that the detection probability was higher when sensors were deployed following the Gaussian distribution instead of the uniform distribution. The reason is that the sensors deployed following a Gaussian distribution tend to concentrate at the center, they are more likely to detect the intruder than the sensors deployed following the uniform distribution when the intruder is close to the target.

B. Effect of Randomly Destroying

In this subsection, we used the same parameters as those for case one. We set the destroy probability to 0.5 without considering the relative position or other factors. Fig. 12 shows

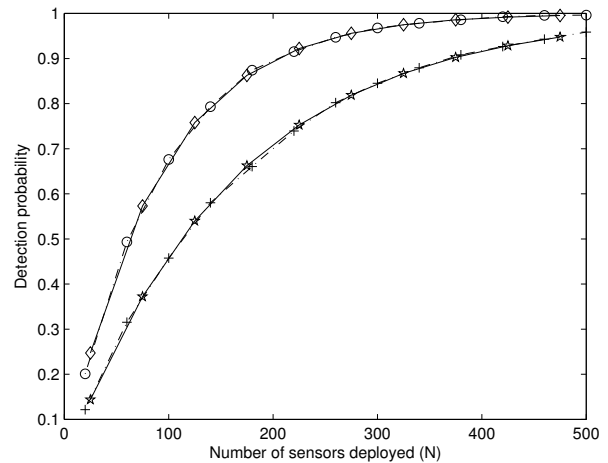


Fig. 10. Detection probability corresponding to the single-sensing detection model when $V = 2.5 \text{ m/s}$.

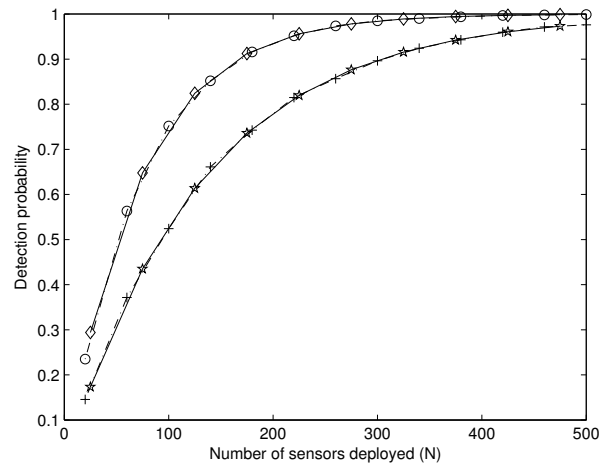


Fig. 11. Detection probability corresponding to the single-sensing detection model when $V = 1.5 \text{ m/s}$.

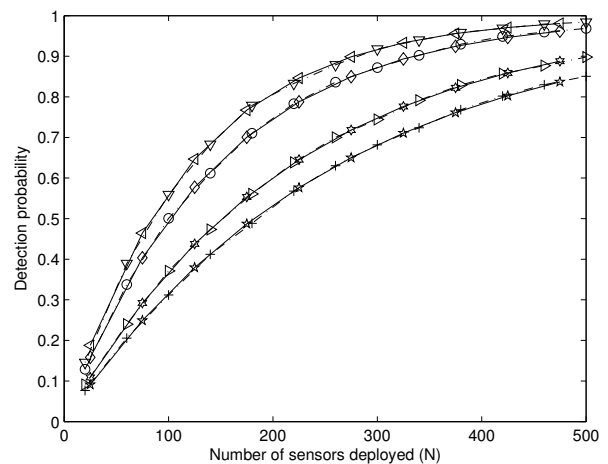


Fig. 12. Detection probability of randomly destroying intruder corresponding to the single-sensing when $V = 5 \text{ m/s}$. Additional legends: solid line+triangle (left): analytical randomly destroying & gaussian, solid line+hexagram: analytical randomly destroying & uniform; dashed line+triangle (down): Monte-Carlo randomly destroying & gaussian, dashed line+triangle (right): Monte-Carlo randomly destroying & uniform.

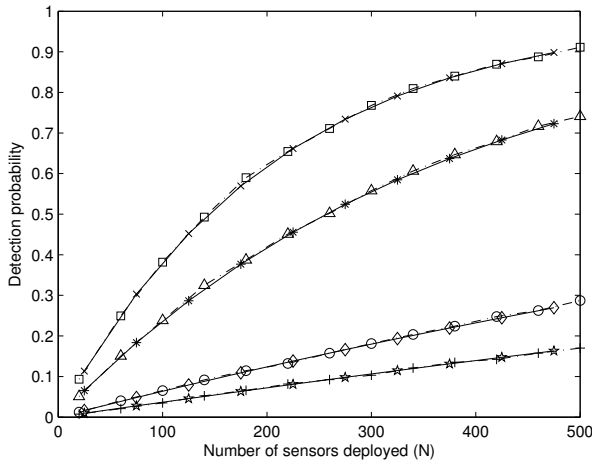


Fig. 13. Detection probability of different identification functions corresponding to the single-sensing when $V = 10 \text{ m/s}$. Solid line+diamond: analytical $\sigma = 1$ & gaussian, solid line+pentagram: analytical $\sigma = 1$ & uniform, solid line+x-mark: analytical $\sigma = 2$ & gaussian, solid line+star: analytical $\sigma = 2$ & uniform; dashed line+circle: Monte-Carlo $\sigma = 1$ & gaussian, dashed line+plus: Monte-Carlo $\sigma = 1$ & uniform, dashed line+square: Monte-Carlo $\sigma = 2$ & gaussian, dashed line+triangle (up): Monte-Carlo $\sigma = 2$ & uniform.

that randomly destroying resulted in the increased detection probability compared to completely destroying. Furthermore, lower random destroy probability leads to the higher detection probability. When the random destroy probability drops to 0, the intruder will not destroy any sensor. The detection probability of the intruder that does not destroy sensors is higher than the detection probability of the destructive intruder (Fig. 12). Due to space limitation, we do not demonstrate the figure of this kind of intruder.

C. Effect of Identification Function $g_{xy}(iT)$

The effect of the identification function $g_{xy}(iT)$ was also investigated in the simulations. The two functions used in our simulations were

$$g_{xy}(iT) = \text{erfc}\left(\frac{\sqrt{(x - R + iTV)^2 + y^2}}{\sqrt{2}\sigma}\right) = \frac{2}{\sqrt{\pi}} \int_{\frac{\sqrt{(x - R + iTV)^2 + y^2}}{\sqrt{2}\sigma}}^{\infty} e^{-t^2} dt \quad (19)$$

where $\sigma = 1$ and $\sigma = 2$. In the simulations, we set the speed of the intruder to $V = 10 \text{ m/s}$. We also changed the detection radius of sensors accordingly. Since the identification functions we used were very similar to the cumulative distribution function (CDF) of a normal distribution, we set the radius of the detection discs to $r_s = 3\sigma$, which was 3m and 6m for $\sigma = 1$ and $\sigma = 2$ respectively. Therefore, the probability that a sensor can identify an intruder outside its detection region is nearly zero. Then, we set to 0 the probability that a sensor located outside of the detection discs identifies the intruder and calculate the detection probability only with the sensors locating inside the detection discs. According to the discussion in Section IV, the simulations with $\sigma = 1$ correspond to case one while the simulations with $\sigma = 2$ correspond to case three.

Comparing Fig. 13 with Fig. 8 and 10, we found that

the identification function decreased the detection probability. The $g_{xy}(iT)$ with the smaller σ resulted in the lower detection probability. The reason is that the detection radius corresponding to a smaller σ is shorter than the detection radius corresponding to a larger σ . As the destruction region is fixed, more sensors, which may sense the intruder, will survive when σ is larger.

VIII. CONCLUSION

In this paper, we have investigated the intrusion detection problem, in which the intruder can destroy sensors in its surrounding region. This new problem was solved through theoretical analysis and our theoretical results were verified through simulations. Moreover, both of the theoretical and experimental results show that the detection probability was lower when the intruder could destroy sensors. We also found that the detection probability was higher when sensors were deployed according to a Gaussian distribution instead of a uniform distribution.

REFERENCES

- [1] D. P. Agrawal and Q. A. Zeng, *Introduction to wireless and mobile systems*, 3rd ed. Independence, KY: Cengage Learning, 2010.
- [2] Y. Wang, W. Fu, and D. P. Agrawal, "Gaussian versus uniform distribution for intrusion detection in wireless sensor networks," *IEEE Trans. Parallel Distrib.*, vol. 24, no. 2, pp. 342-355, Feb. 2013.
- [3] Y. Wang, X. Wang, B. Xie, D. Wang, and D. P. Agrawal, "Intrusion detection in homogeneous and heterogeneous wireless sensor networks," *IEEE Trans. Mobile Comput.*, vol. 7, no. 6, pp. 698-711, June 2008.
- [4] R. Tan, G. Xing, J. Wang, and B. Liu, "Performance analysis of real-time detection in fusion-based sensor networks," *IEEE Trans. Parallel Distrib.*, vol. 22, no. 9, pp. 1564-1577, Sept. 2011.
- [5] X. Liang and Y. Xiao, "Mobile sensor intrusion detection under any shape of curve," *Math. Comput. Modelling*, vol. 57, no. 11-12, pp. 2904-2917, June 2013.
- [6] I. Butun, S. D. Morgera, and R. Sankar, "A Survey of Intrusion Detection Systems in Wireless Sensor Networks," *IEEE Commun. Surveys Tuts.*, vol. 16, no. 1, pp. 266-282, First Quarter 2014.
- [7] S. Capkun, M. Hamdi, and J. Hubaux, "GPS-free positioning in mobile ad-hoc networks," in *Proc. of the 34th Ann. Hawaii Intl Conf. System Sciences*, Jan. 2001.
- [8] Y. Wang, X. Wang, D. Wang, and D. P. Agrawal, "Localization algorithm using expected hop progress in wireless sensor networks," in *Proc. of the 3rd IEEE Intl Conf. Mobile Ad hoc and Sensor Systems (MASS 06)*, Vancouver, Canada, Oct. 2006, pp. 348-357.
- [9] N. Katneni, V. Pandit, H. Li, and D. P. Agrawal, "Hybrid gaussian-ring deployment for intrusion detection in wireless sensor networks," in *IEEE Int. Conf. Commun. (ICC)*, Ottawa, Canada, June 2012, pp. 549-553.
- [10] Y. Wang and Z. Lun, "Intrusion detection in a k-gaussian distributed wireless sensor network," *J. Parallel Distrib. Comput.*, vol. 71, no. 12, pp. 1598-1607, Dec. 2011.